A purely bioinformatic pipeline for the prediction of mammalian odorant receptor gene enhancers

EPS architecture analysis for future high-power missions

Christopher A. Paissoni[1] and Nicole Viola[2]
Department of Mechanical and Aerospace Engineering, Politecnico di Torino, Turin, Italy,10129

Tommaso Andreussi[3], Alena Kitaeva[4] and Mariano Andrenucci[5]
Sitael S.p.A., Via Alessandro Gherardesca, 5, Ospedaletto (PI), Italy, 56121

The space tug can represent a valid solution to provide transportation capabilities for future space missions. In particular, the tug can be effectively adopted for different applications such as electric orbit raising for commercial satellites and cargo transfer to resupply space infrastructures. The adoption of high-power electric propulsion is a fundamental enabler for these typologies of mission owing to its advantages in terms of long lifetime, high performance and operational flexibility. However, further investigation should be performed in order to optimize the design of the space tug considering different architecture alternatives. We defined two sets of thruster operative points for a more representative comparison of EPS architecture cases. In particular, we analyzed three aspects: the adoption of a cluster of thrusters vs the monolithic approach; the implementation of a direct drive power supply vs the traditional power processing unit; the selection of krypton propellant vs xenon.
The design of the space tug is performed with MAGENTO tool, a design software developed in a collaboration between SIATEL and Politecnico di Torino in the framework of an ESA GSTP project. The results of the design phase are compared by mean of the analytical hierarchy process to identify the optimal design solution for the spacecraft design.

I.Introduction

In the recent years, High Power Electric Propulsion (HP-EP) has been identified as the most promising technology for enabling new and more challenging frontier in expansion of human presence in space. A vast majority of the research activities on HP-EP is now focused on the development and qualification of High-Power Hall Thruster (HP-HT), selected among the EP technology as the most suitable for future applications. Several HP-HTs were developed and tested to investigate the operational features of these thrusters. In Europe, SITAEL is one of the main actors in high-power thruster-class field with the development of a 5kW-class and 20kW-class thruster, respectively the HT5k [1] and the HT20k [2].
These thrusters can benefit to mid and long-term space applications, in different operative environments. In particular, this technology is envisaged to be used on-board: (i) large telecommunication and navigation satellites to perform electric orbit raising (EOR) manoeuvres to reach the final operative orbit, (ii) space transportation systems, to perform the transfer of cargo and supply materials between two orbits, (iii) for service platforms, to provide thrust mainly for both refuelling and deorbiting/disposal of platforms, (iv) for exploration and scientific platforms, as primary propulsion.

[1] PhD Student, Department of Mechanical and Aerospace Engineering, Politecnico di Torino, christopher.paissoni@polito.it, AIAA student member.
[2] Associate Professor, Department of Mechanical and Aerospace Engineering, Politecnico di Torino, nicole.viola@polito.it, AIAA member.
[3] Technical Manager, Space Propulsion Division, tommaso.andreussi@sitael.com.
[4] EP research engineer, Space Propulsion Division, alena.kitaeva@sitael.com.
[5] Head, Space Propulsion Division, mariano.andrenucci@sitael.com.

In order to implement more sustainable and affordable space missions, new transportation systems could be developed enhancing specific capabilities such as their reusability, to exploit them for more than one transfer, and their operational versatility, to use them for different purposes. These capabilities can converge in the adoption of a space tug, a reusable transportation system able to perform end to end transfers between two orbits. The payload transferred by the space tug could be identified either in a commercial satellite, to be transferred in its target operative orbit or in a cargo module, to resupply a space infrastructure such as a space station or an orbital refuelling station.
Taking into account these properties during the design phase, this typology of system will allow to reduce the mission cost, increasing mission sustainability and affordability with respect a possible future evolution of the chemical-based transportation system.
In previous works [3][4] all the applications listed have been analysed in different environments, identified in accordance with the Global Exploration Roadmap (GER2018) [5]. This process resulted in the development of 33 mission concepts each one characterized under both the system and the operational point of view. The starting and the target orbits, the refuelling orbit, the cargo mass transferred, and the traffic plan assumed, as well as the maximum transfer time were defined for each of the mission scenario identified. The HT20k was selected as reference thruster to be adopted on-board any of the platforms. The outcomes of these preliminary analyses were used to select a region on the operational envelope of the thruster where the majority of the mission concepts introduced turned out to fulfil the mission requirements and constrains defined during the mission analysis. However, few criticalities were identified in particular related to the system budgets. In order to perform multiple transfers, the space tug required a high propellant mass as well as the introduction of either dedicated systems or an infrastructure to provide refuelling capability in according to the selected refuelling strategy. Furthermore, the adoption of HP-HT required the generation of high power and the consequent dissipation of high heat loads derived from its processing. Lastly, for the fulfilment of the imposed mission requirements, a “high thrust” level was required.

This paper investigates possible solutions to mitigate these criticalities. Specifically, three different design choice were selected:

1) Monolithic vs cluster EPS architecture: the subsystem can be based on a single EPS string or multiple, string with a lower power. The cluster solutions can provide high-thrust level increasing the overall reliability of the EPS.
2) Kr vs Xe propellant operations: the adoption of different propellant could bring benefit in terms of costs even if different storing conditions shall be carefully investigated.
3) Direct Drive vs traditional PPU architecture: instead of feeding the thruster through a Power Processing Unit (PPU), a Direct Drive Unit (DDU) can be used. This has direct and indirect effects at system at subsystem level on all the operations.

The present analysis was performed in the framework of the EU’s H2020 Consortium for Hall Effect Orbital Propulsion System (CHEOPS) programme and an ESA\GSTP project with the MultidisplinAry desiGN Electric Tug Tool (MAGNETO) tool [6], an upgraded version of the previous MISS toll, developed by Politecnico di Torino.

To investigate the adoption of the architecture alternatives previously listed, highlighting advantages and disadvantages in their adoption, a reference mission scenario was introduced. It consists in a transfer of a 2 tons commercial telecommunication satellite from its injection Low Earth Orbit (LEO) up to its final operative Geostationary Earth orbit (GEO). This typology of mission is still under particular attention by the operators due to the economic interest behind the possibility to provide telecom capabilities reducing the transfer costs. With the aim of comparing and identifying an optimal design solution, a trade-off process based on the Analytical Hierarchy Process (AHP) was implemented.

In this paper, after a detailed description of the alternative architecture under analysis and the definition of the thruster operative point considered (section III), the mission analysis performed on the selected reference transfer will be presented. After that, the design process based on MAGNETO tool will be detailed in section IV focusing on the upgrade of the design module necessary to assess the impacts of the alternative architecture on the platform design. The trade-off process definition along with the results obtained will be than presented in section V. Finally, section VI will report the main conclusion and the further developments of this analysis.

II.Mission profile

As previously defined, the different design solutions were studied analyzing their effects at mission, system and subsystem level through the definition of a reference scenario hereafter presented. The space tug could represent a valid alternative to the classical design solutions owing to its intrinsic characteristic of reusability and versatility. This allow to develop a mission concept where cyclical transfers between two orbits are envisaged. As a consequence, the reference mission was based on a LEO to GEO transfer of a commercial telecommunication satellite. The mass of the satellite was fixed at 2 tons, considering the recent trend of reducing the GEO platform mass with the launch of platform such as Small GEO and ELECTRA [7][8]:

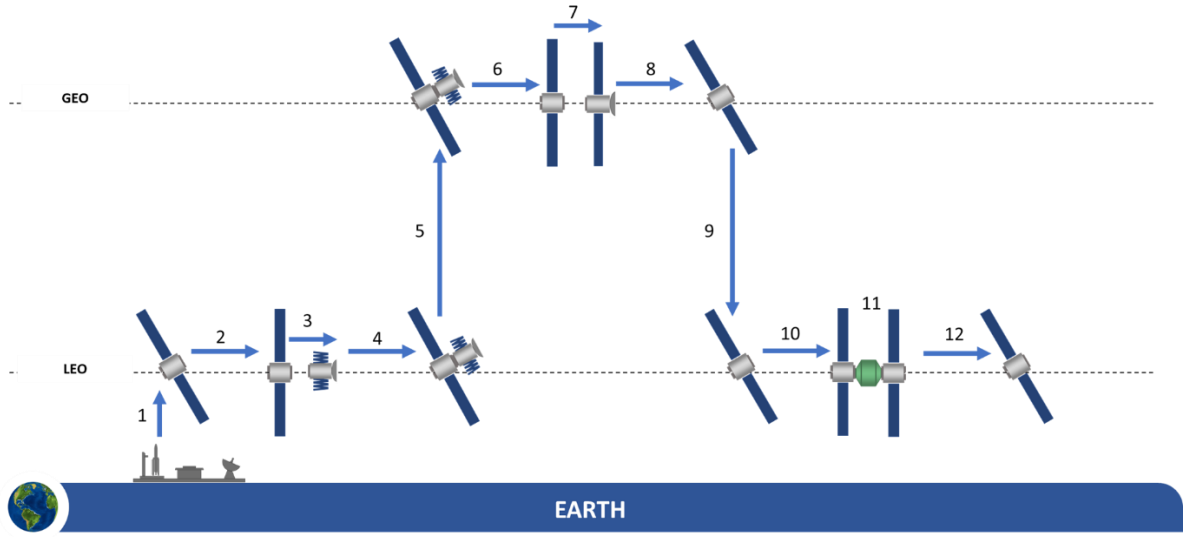

Figure 1: Design reference Mission (DRM) of the LEO-GEO transfer reference mission.

Figure 1 shows the mission profile selected as the reference scenario for the investigation of the different architecture cases. After its launch into orbit, the space tug waits on a LEO parking orbit, waiting for the launch of the telecommunication satellite to be transferred. Then, in order to perform the rendezvous and docking (RVD) manoeuvre with the target telecommunication satellite, it has to assess its relative position with respect to the target telecom satellite. Once the RVD manoeuvre is concluded, the space tug has to wait the GO-command to perform the transfer up to the final GEO position defined by the operative requirements of the telecom satellite. When this position is reached, the tug releases the telecom satellite and performs a disengaging manoeuvre to move toward a safety position and starting the electric transfer phase back to the LEO parking orbit. Reaching the initial parking orbit, the space tug has to wait for the following launch of a telecom satellite to be transferred. During this waiting period, the refuelling operations take place through the availability of an On-orbit Refuelling System (ORS) which will be launched on the tug LEO parking orbit.

The refuelling operations are assumed to be performed at the end of every transfer in order to reduce the propellant mass unexploited during the transfer to GEO and, consequently, optimized the propellant consumptions.

Moreover, it is important to highlight that the space tug will be equipped with a chemical propulsion subsystem acting as actuators for the Attitude and Orbit Control Subsystem (AOCS). This subsystem is also used for the RVD manoeuvre in order to allow contingency manoeuvre for collision avoidance and to limit the degradation effects caused by plume impingement and contamination of the plasma beam, generated by the tug thrusters.

III.ARCHITECTURE SOLUTIONS

a. Monolithic vs Cluster

To equip a spacecraft with a 15-25kW electric propulsion subsystem, it is possible to follow two different approaches:

1) Clustering 5 kW-class thruster units,
2) Using of a single monolithic 20 kW-class thruster.

Whereas the implementation of clustering may obviate the need to use thruster orientation mechanism (TOM), the monolithic option necessarily requires the application of TOM. This necessity complicates the thruster integration onto the thruster platform and may have some impacts on the thermal management of the system.

Nevertheless, the clustering approach introduces several complexities in system integration, validation and operation, and the overall performance of the propulsion subsystem is typically lower than that of a monolithic thruster. As a matter of fact, to produce the same level of thrust, the cluster solution requires higher power levels with respect to the monolithic solution. This implies larger thrust-to-power ratios for the cluster option. Additionally, since higher power-level thrusters are intrinsically more efficient, the difference in the overall efficiency becomes more relevant when comparing a cluster of 5 kW thrusters with a single 20kW device.

Moreover, direct sputtering erosion of inactive thrusters caused by firing of the active ones, is a great drawback of clustering, in particular for long operation times. Moreover, the clustering approach leads to a higher number of components leads to a greater complexity at system level, in particular for what concerns its (i) integration on the platform, due to the complex arrangement of the components, (ii) validation, due to the difficulties in testing a cluster and, (iii) operation, due to the complex thrust steering law to implement in order to avoid residual torque momentum on the spacecraft.

The integration of a cluster is more complex with respect to the monolithic approach due to the greater number of components that have to fit inside a spacecraft. Moreover, the thruster arrangement has to be carefully evaluated in order to avoid thrust misalignment intrinsically derived from the geometrical disposition of the thrusters. Other aspects related to the integration complexity can be identified in the greater impact on the Thermal Control System (TCS) which has to manage heat flux generated by multiple hot spots.

The greater number of components and the possible cross-effects between them, leads to more complex validation processes which could require specific procedures, tools and, facilities.

Furthermore, the clustering approach introduces a greater flexibility in operation owing to the possibility to control independently each single EPS string. In some particular cases, this allows to obviate the use of thruster orientation mechanisms (TOM), controlling the thrust vector through an appropriate throttling of the thrusters. Furthermore, considering the throttling range of the single EPS string, a greater thrust range is obtainable. However, on the other side the increasing in the EPS operation flexibility is the greater complexity of the EPS control logic which has to be implemented for the cluster architectures with respect to the monolithic architectures.

b. PPU vs DDU

The conventional solution for EP systems is to use a power-processing unit (PPU) to modulate the energy produced onboard to meet the requirements necessary for Hall thruster operation in terms of current and voltage. Although PPUs have been used successfully in several space missions, one main drawback of these units is their relatively large size and mass. Apart from introducing an efficiency loss, the high power PPUs produce a significant amount of heat and therefore increase the workload of the spacecraft thermal management subsystem.
Another solution to deliver power to the Hall thruster is to directly transfer the energy generated by solar arrays to the thruster. This approach, which is called “Direct-Drive (DD)”, allows simplifying the PPU greatly, removing all power converters and implementing a simplified filter unit on the anode power line.
However, to benefit from the positive aspects of the direct-drive approach, it is necessary to develop satellite platforms with high bus voltages in the range of 300 to 500V, requiring high-voltage solar arrays and power bus. Moreover, the application of the high bus voltages implies that the satellite platforms would be more vulnerable to damages caused

by charging. In addition, the PPU in conventional electric schemes serves as a galvanic isolator. Thus, non-isolated connection of the thruster to the solar arrays in the direct-drive scheme necessitates using appropriate filter units to damp out the possible large-amplitude oscillations in the thruster's discharge current.

In addition, the implementation of the DD approach necessitates the incorporation of new components in the spacecraft power system architecture, such as cathode return potential (CRP) power supply [9].
On a heritage perspective, SITAEL has performed an extensive experimental campaign aimed at characterizing the controllability and stability of operation of its HT5k LL thruster using the direct-drive approach. One objective of the tests carried out was to quantify the values of CRP, which influences the amount of detrimental beam stray current towards spacecraft bus. Furthermore, three different control algorithms were developed and tested. The effectiveness of these algorithms in regulating the thruster behaviour was verified against representative variations in I-V characteristic curves of a solar array simulator.
Compared to the tests performed in SITAEL on the HT5k LL using conventional power supplies, the general conclusion from the experiments on the direct-drive HT5k LL was that no major differences exist in operating the thruster using the direct-drive approach.

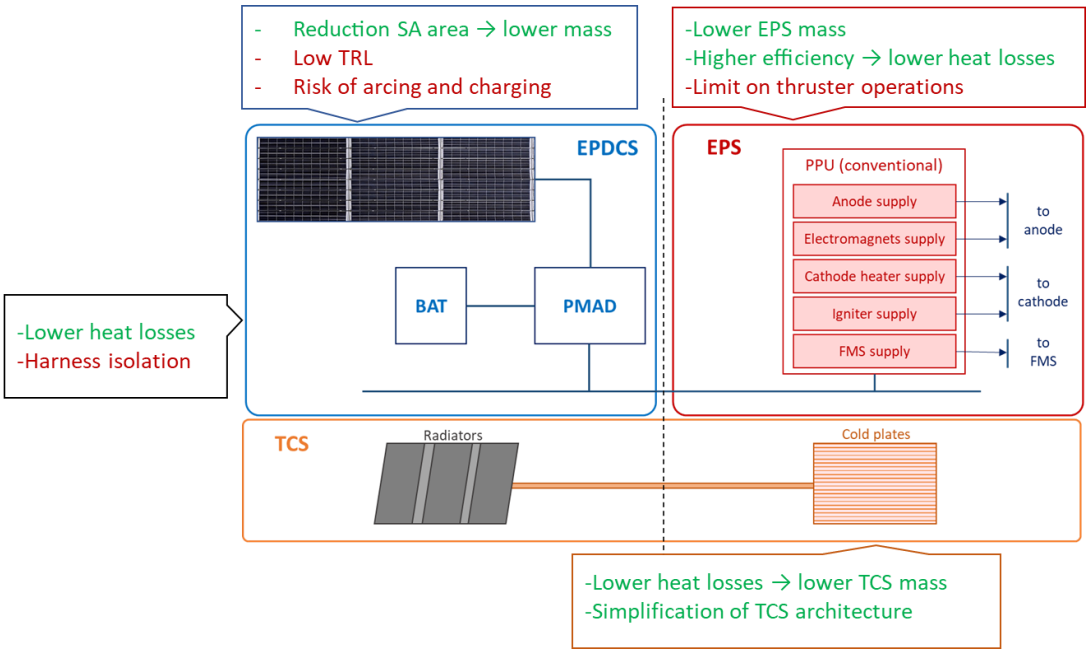

Figure 2: schematic representation of advantages/disadvantages of the DDU implementation subdivided with respect to the subsystems mainly affected.

c. Xenon vs Krypton

Krypton has physical properties close to those of Xe and a similar non-corrosive nature. These features, associated with krypton lower price, make it one of the most likely alternative propellants for the HET-based EPS, in particular for missions with high total impulse. The price of krypton is up to eighteen times lower than of xenon (Xe cost: 2200 €/kg, Kr cost: 120 €/kg [Latest quotation 01/2019]). However, due to its lower atomic mass with respect to xenon, the specific impulse for operation with krypton at the same voltage and power level is higher whereas the thrust is lower. SITAEL has already accomplished extensive experimental characterization of Hall thruster performance and behavior with krypton. Krypton was used during the test campaigns with two Hall thrusters of different power levels, 5kW-class and 20kW-class. In particular, a dedicated series of tests have been performed under the ESA ARTES 5.1 program element to characterize the performance and erosion of the SITAEL's HT5k thruster [10]. The operation with krypton showed a reduction in thrust and efficiency in parallel to an increase in specific impulse.

Another consequence of krypton lower atomic mass is reflected in terms of increased beam divergence. The beam divergence efficiency, when operated with Kr was reported to be 8% lower than with Xe [11]. Furthermore, due to the lower first ionization potential and higher ionization rate already at lower electron energies, Xe provides lower ionization cost and higher propellant utilization efficiency. At the same mass flow rate the propellant utilization for Xe was reported to be 5-10% better than for Kr [12]. As a result, the thrust-to-power ratio is typically lower for krypton. From the point of view of the plasma-wall interactions, compared to xenon, the krypton ions are accelerated to higher velocities in the same potential drop and, at the typical ion energies of HETs, the sputtering yield of the wall material increases for lighter particles. Hence, the erosion problem exacerbates with krypton. Moreover, in SITAEL, the HC20 and HC60 cathodes, originally developed for Xe, were tested also with Kr. The cathodes proved to be completely compatible with Kr but operated with higher power consumption, due to the higher ionization energy of Kr [12].
Based on the experimental results from these experimental campaigns and using the scaling model developed by Shagayda [13] the anodic specific impulse can be presented as a function of thrust**Error! Reference source not found.** for different power and discharge voltage levels.

What concerns system level aspects, xenon exhibits the high boiling point and high density at fixed pressure level. Therefore, it features a better storability than other potential propellants including krypton. To obtain Kr storage density above 1 kg/dm3, the krypton shall be stored at pressure above 250 bar, which implies higher challenges to the fluidic system and higher tankage fraction. However, the critical temperature of Krypton (Tcr, Kr = -63° C, Tcr, Xe = 17° C), provides a significant advantage from the point of view of thermal control.

d. Investigated architecture alternatives

The adoption of these alternatives was investigated considering a set of possible system architectures, representative for a trade-off analysis. The following table reports the selected cases:

Table 1: alternative cases under analysis.

	MONOLITHIC	CLUSTER	PPU	DDU	XENON	KRYPTON	
1	X		X		X		CASE#1
2	X		X			X	CASE#2
3	X			X	X		CASE#3
4		X	X		X		CASE#4

Starting from the baseline requirements previously defined two different sets of operative points for HT20k and HT5k thruster were identified and analysed for the architecture cases reported in Table 1. The two sets were chosen for better illustration of the effects of different parameters on the trade-off results and can be selected depending on the mission constrains and customer needs. Each of the four cases from Table 1 was analyzed then for both sets.
For the SET-1, the approach was to fix the values of the specific impulse and total EPS thrust. The corresponding thrust for each of the 5 kW thrusters in the cluster architecture was considered equal to 25% of the monolithic 20-kW one. The corresponding voltages and power discharge power level for both propellants were obtained from the SITAEL HT20k and HT5K performance maps. As expected, the discharge voltage for the same thrust/specific impulse combination is lower for the system operating on Kr, while the discharge power is higher, due to the higher ionization losses with respect to the Xe case.

Table 2: first set of thruster operative points.

SET-1	POWER [kW]	THRUST [mN]	SPECIFIC IMPULSE [s]	VOLTAGE [V]	PROPELLANT MASS FLOWRATE [mg/s]
HT20k Xe	21	1	2500	450	40.5
HT20k Kr	22,5	1	2500	375	40.5
HT20k Xe DDU	21	1	2500	450	40.5

HT5k Xe	6	0,25	2250	600	10.2

For the SET-2, the voltage and the total EPS power were fixed. For the cluster approach the power to each thruster was considered as 25% of the total power available for the EPS. The corresponding discharge power, thrust and specific impulse is presented in Table 3.
Due to the higher efficiency of the electrical sub-system, the Direct Drive approach allows higher power to be utilized for the plasma discharge and consequently higher thrust and specific impulse for the same operative voltage.
EPS on Kr with a traditional PPU provides higher specific impulse, lower thrust and lower mass flow rates with respect to the one on Xe.

Table 3: second set of thruster operative point.

SET-2	POWER [kW]	THRUST [mN]	SPECIFIC IMPULSE [s]	VOLTAGE [V]	PROPELLANT MASS FLOWRATE [mg/s]
HT20k Xe	21	1	2500	450	40.5
HT20k Kr	21	0,77	3000	450	26.4
HT20k Xe DDU	22,2	1,06	2550	450	42.4
HT5k Xe	5,25	0,26	2130	450	12.4

IV.Analysis process

After the identification of the mission scenario and its characterization in terms of functionalities, mission phases and operations, the system design definition proceeds with the sizing of the platform and its subsystems. For this step, an upgraded version of MISS tool has been developed and called MultidisplinAry desiGN Electric Tug Tool (MAGNETO) [6]. After the introduction of the main tool structure, a detailed description of the design models necessary to investigate the adoption of the alternative architectures under study is reported. These models were implemented in the sizing routines of MAGNETO.

A. MAGNETO tool

This software is a multi-input/output design tool which allows to define the mission scenario considering mission requirements and constrains derived from the mission definition phase. The general architecture of MAGNETO tool is shown in Figure 3.

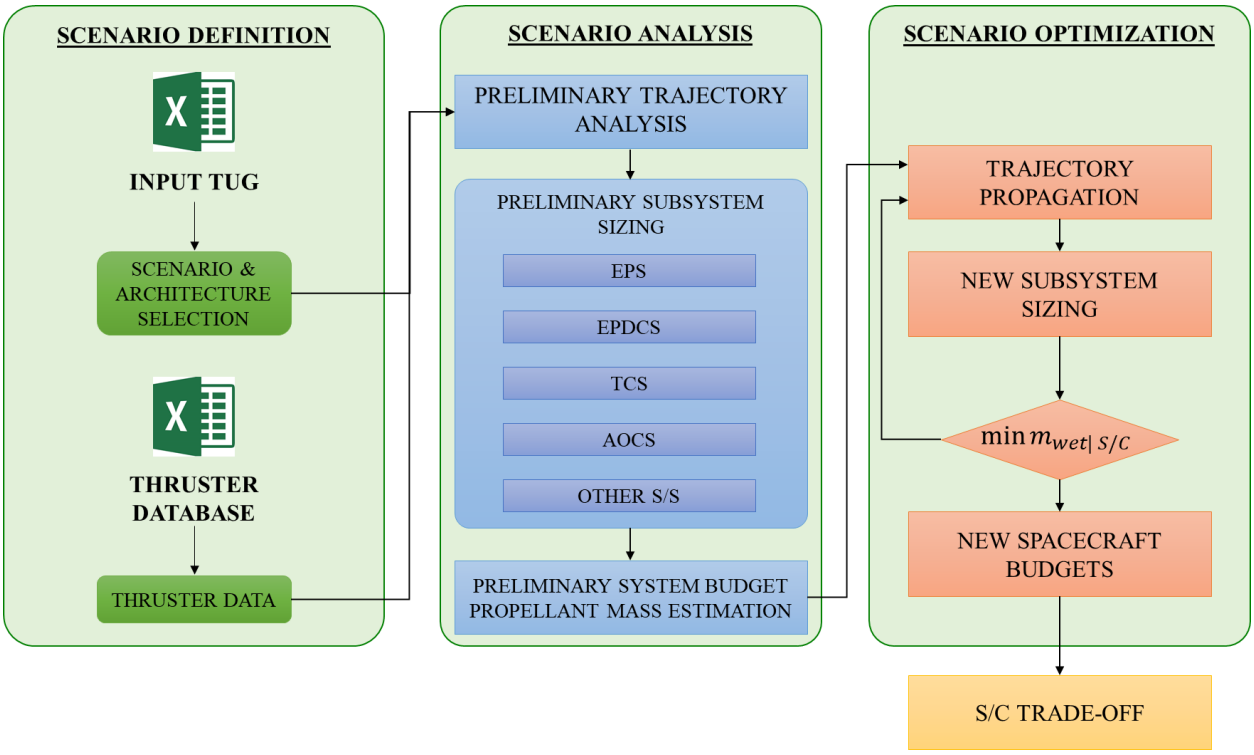

Figure 3: simplified structure of MAGNETO tool.

MAGNETO is based on three main modules: (i) scenario definition, (ii) scenario analysis and (iii) scenario optimization. In the first module, the mission scenario is introduced uploading two main database. The first of them contains the subsystem design inputs through which the architecture of the different subsystems is defined, along with the identification and characterization of the mission phases. In particular, for what concern the characterization of the mission phases, they are defined in terms of: (a) initial and final orbital values, (b) phase during which the telecom satellite is transferred and its mass, (c) maximum duration of the phase (for waiting phases only), (d) location of the refuelling operation and mass of propellant transferred.
During the scenario definition phase, the second database uploaded contains all the operative envelope of the thrusters considered. In fact, the tool has the possibility to analyse the operation of different typologies of HT, defining power level, thrust, specific impulse, propellant mass flow rate and voltage level for each desired operative point over the thruster operational map.
After the definition of both scenario and design input data, the initial design of the tug is performed in *Mission Analysis* module, where the main mission and system budgets are calculated. This preliminary sizing is based on "classical" subsystem models derived from [14], tailored with respect the peculiarities introduced by the adoption of the electric propulsion technology. In particular, for what concerns the EPS sizing, it is possible either to select the data stored in a mass breakdown, if the thruster is known, or based its sizing on a parametric model derived from a database of thruster. These two different approaches are also exploited for the sizing of the other components of an EPS string, such as: Power and Processing Unit (PPU), tank, pressure management assembly (PMA) and Flow Control Unit (FCU).

Furthermore, particular attention is given to the Electric Power Distribution and Control Subsystem (EPDCS) and to the Thermal Control Subsystem (TCS) and the Attitude and Orbit Control Subsystem (AOCS). First, the EPS is designed considering the power budget of the tug during all the mission. The power generation function is in charge of solar arrays sized in terms of geometry and mass requirements. The batteries are instead considered for the storage of electrical power during eclipse period. Their sizing considers inputs coming from both the previous tool module and the preliminary analysis of the trajectories considering the worst case. The AOCS and the TCS are sized considering the environmental conditions in which the tug has to operate. This allows to define the budgets of the system comprising passive components, actuators and sensors.

This sizing phase is exploited in order to provide initial value for an optimization process performed in the last module of MAGNETO. In the *System Optimization* module, an iterative process allows to refine the mass of the spacecraft and optimized the propellant mass to be stored onboard the tug that affects the design of the tanks. Specifically, this optimization is performed exploiting a sequential algorithm, nested in an iterative cycle, able to identify the manoeuvres to perform during a specific phase and propagate the trajectory considering an imposed steering control law to identify the direction of thrust vector.
A set of weights for each orbital parameter is derived taking into account the values of the orbital parameters at each integration step, averaged by the difference between their initial and final values. This thrust steering law allows to obtain a suboptimal solution as demonstrated in [6]. After the propagation of the trajectories performed for each phase, the spacecraft is sized again in order to update the all the budgets. This process is then repeated up to convergence of the spacecraft wet mass within a determine tolerance range. The results obtained from the MAGNETO tool are compared through a trade-off analysis during the post-processing phase where a set of figures of merit (FoM) is evaluated in order to select the optimal system architecture.

B. DDU design model

The DDU architecture design process is based on several modules introduced in the design process of the subsystems mainly affected by this peculiar system configuration, such as the EPS, the TCS, and the EPDCS. Following a general subdivision between direct and indirect effects, the modules introduced are here presented. In particular, the direct effects are identified as those directly affected the EPS. The indirect effects are instead those not directly related to the adoption of a DDU architecture but rather deriving for specific design choices in the design of the spacecraft not necessary based this architecture,

- *Direct effects of Direct Drive implementation on EPS*

For what concern the EPS, the main benefit of the DDU architecture with respect to the conventional PPU is the removal of the anode module(s). The mass savings provided by the DDU system can be, thus, evaluated as the difference in mass with respect to a classical PPU configuration. In addition to the anode module mass saving, the PPU mass is further reduced owing to the smaller dimensions of both the chassis and the size of the TCS components necessary to dissipate the thermal load generated by the electronic components.

First, the anode module is designed as a single module of a conventional PPU in terms of a DC-DC converter, considered to be constituted by: (i) a chopper stage, which converts fixed DC input to a variable DC output voltage, (ii) an inverter transformer stage, to change the voltage output and provide isolation between input and output load, and (iii) a rectifier stage that provides rectified AC current to (iv) a downstream DC filter, whose output is a DC current to the Thruster Unit. A DC filter is placed upstream of all components to isolate the EPS from the EPDCS.

Figure 4 shows the conceptual arrangement of the components that form the PPU anode module.

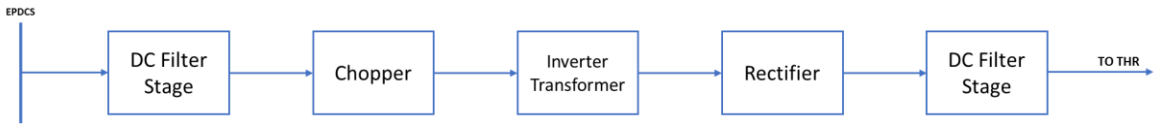

Figure 4: Conceptual physical block diagram of a conventional PPU.

To estimate the mass of a single anodic module, the model developed by NASA Glenn Research Center is used [15]. This model provides the mass trend evaluation of all electronic components, which constitute an EPS of a spacecraft, with respect to their sizing variables. Considering the models related to the components in Figure 4, the overall anodic module mass is obtained by summing over the corresponding mass of all components.

The design parameters introduced for the sizing of the electronic stages considered are hereafter listed:

- DC Filter stages: the input/output filter voltages and powers, the ripple factor, the filter efficiency (assumed equal to 99.8%), the switching frequency (assumed equal to 100 kHz) and the available/required module to define the internal redundancy logic (assumed equal to 3 required modules and 4 available modules assumed);
- Chopper stage: the input/output voltages and power levels, the switching frequency derived for the suggested values on [15], and the available/required modules assumed (3 required and 4 available modules assumed);
- Inverter/transformer stages: the input/output voltages and power levels, the switching frequency (in kHz) derived for the suggested values on [15], and the available/required modules assumed (3 required and 4 available modules assumed);
- Rectifier stage: the input power and voltage level, the stage efficiency (assumed equal to 98,7 % for stages operating over 110V) and the required available modules (3 required and 4 available modules assumed)

The Switching Frequency (SF) for both the Chopper and the Inverter/Transformer were derived using the suggested values in [**Error! Reference source not found.**].

Another main advantage of the DDU system implementation is the reduction in mass of the TCS. As previously mentioned, the higher efficiency of the DDU system lowers the generated heat that needs to be dissipated by the TCS, which reduces the mass of the components necessary to collect transport and dissipate the heat loads. In particular, the design solution usually adopted for the conventional PPU architectures consists of heat pipe loops through which the heat flux generated by the PPU flows to either deployable or body-mounted radiators. In some specific architectures, the PPU is placed in contact with body-mounted radiators, therefore, avoiding the adoption of heat pipes loops. Due to the preliminary approach of the TCS design, the scheme with the heat pipe loops connected with body mounted radiators is considered. The TCS mass saving is assessed considering an average power specific mass of 28 kg/kW for the radiators and 14 kg/kW for the heat pipes loops [14].

- *Indirect effects of Direct Drive implementation on other subsystems*

As briefly discussed in the section III, the indirect advantages are those that are not directly linked with the implementation of a DD scheme. These advantages are, in fact, due to design solutions that can be implemented regardless of the EPS architecture. In this respect, the design of a high-voltage Electric Power Distribution and Control Subsystem (EPDCS), which provides high-voltage power to the EPS as well as to other subsystems on-board a spacecraft, can serve as a major source of mass and cost benefits. However, in spite of several advantages that may be obtained, some technological limitations exist that should be carefully investigated and will be described later.
The present analysis in this section considers only the effects and gains related to the adoption of high-voltage solar arrays and batteries, as components of a high-voltage EPDCS. All subsystems are supposed to be supplied by a high-voltage bus for their operation avoiding the increment in weight due to a step-down converter.

- *High-voltage solar arrays*

The selection of a high-voltage power bus necessitates the use of high-voltage solar arrays (SA). Despite the issues caused by the plasma environment surrounding the SA, as well as possible electric charging and arcing events, the implementation of a DD system allows a notable reduction in the SA area because of the higher efficiency of the DDU, and thus, the consequent reduction in the power demand required from the SA.
A review of the state-of-the-art in high-power SA showed that Ultraflex and Megaflex solar arrays developed by Orbital ATK are suitable for high-voltage operations [16][17] These SAs have a specific architecture of the cells to increase the specific power, thus, increase the scalability to high power levels and feature innovative deployable system based on folding spar joints and panel extension hinges, allowing very high packing efficiency.
In order to estimate the indirect advantage of the DD system coming from the high-voltage SA, the methodology presented in [14] is followed. Table 4 summarizes the design parameters used in the analysis. The SA area was calculated for the power levels required in both the PPU and DDU configuration.

Table 4: SA design parameters.

	PPU configuration	DDU configuration	NOTE
Daylight time [s]	5400		Derived for worst condition in LEO>GEO transfer
Eclipse time [s]	1800		Derived for worst condition in LEO>GEO transfer
Daylight path efficiency (X_D)	0.85		[14]
Eclipse path efficiency (X_E)	0.65		[14]
Cell efficiency (BOL)	33 %		Multijunction GaAS
Inherent degradation	0.805		[14]
Specific power [W/kg]	120		[16][17]

As shown in Table 4, the lower power required by the platform because of DD system higher efficiency and lower losses through the power bus, translates in a reduction of the SA area. This has a direct effect also on the Attitude Orbit and Control Subsystem (AOCS) since the requirements on the torque force that it should counteract will be relaxed, therefore, resulting in the reduction of the subsystem mass. However, this effect is not included in this work.

- *High-voltage battery*

The batteries represent one of the most critical issues for high-voltage EPDCS design. This is because of the fact that on the one hand, high-voltage bus could require several cells in series which increases the design complexity of this subsystem. On the other hand, adopting low-voltage batteries requires the use of a step-down converter. In this case, the subsystem mass savings and the reduction of generated heat load are lowered.
The Li-ion batteries were selected with an energy density of 130 Wh/kg [13]. This adoption of this typology of cells allows to reduce the number of cells necessary to operate at high-voltage level. The design of the batteries considers the worst-case scenario of eclipse during LEO to GEO transfer.
The power to be provided during the eclipse time is assumed to be 10% of the maximum power of the spacecraft. It is also pointed out that if a high-voltage EPDCS is selected, it allows the relaxation of this requirement due to the lower power dissipation of the power bus.
Following the design methodology presented in [13], the design parameters taken into account are reported in Table 5.

Table 5: Battery Design Parameters

	PPU configuration	DDU configuration	NOTE
Eclipse time [s]	1800		
DOD	0.75		[14]
Transmission efficiency	0.9		
Energy density [Wh/kg]	130		[14][**Error! Reference source not found.**18]

- *High-voltage power bus*

Adopting a high-voltage power bus for the EPDCS brings about other advantages at the spacecraft-level. In fact, a higher voltage bus can provide the same power level with a lower current, compared to a lower-voltage bus. Consequently, the ohmic heat dissipations ($P_D = RI^2$) are reduced and thus, less heat shall be managed by the TCS. Assuming that 7% of total power is dissipated as heat [15] for a system based on PPU, the following ratio is defined to derive the power dissipated by a DDU-based system ($P_{D,\,HV}$):

$$\frac{P_{D,HV}}{P_{D,LV}} = \frac{R\,I_{HV}^2}{R\,I_{LV}^2} = \frac{\left(\frac{V_{LV}}{V_{HV}} I_{LV}\right)^2}{I_{LV}^2} = \left(\frac{V_{LV}}{V_{HV}}\right)^2 \tag{1}$$

in which the indexes HV and LV denote High Voltage and Low Voltage, respectively. As another important point, when a high-voltage power bus is selected, it can be also possible to reduce the cross-section of the wires because of the lower current level that they need to carry. This design choice allows reducing the mass of the power bus. However, this design option results in same values of the heat to be dissipated by the TCS. Therefore, reducing the bus mass by selecting smaller-diameter wires or reducing the TCS mass by lowering the ohmic power dissipation in the wires while keeping the wires diameter constant present two design options at the S/C-level. The selection of one option over the other requires more detailed trade-off analyses, beyond the scope of the current high-level analysis. Accordingly, for the purpose of presenting an overall estimate of DD system advantages, and with no further investigations on the spacecraft harness, the design solution of constant wire cross-section is selected.

C. Store alternative propellant

The comparison of Kr and Xe propellant density dependence from the pressure for the temperature of 45°C is presented in Figure 5.

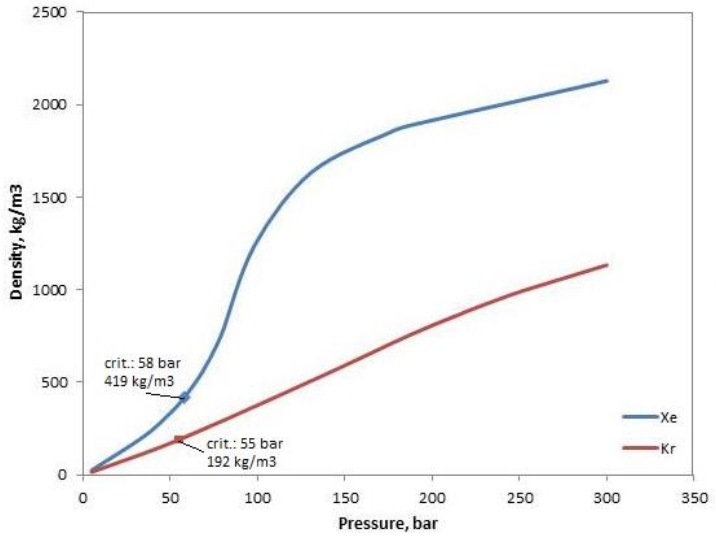

Figure 5: Kr and Xe propellant density vs storage pressure at 45°C.

As it was already mentioned, krypton has a higher tankage fraction (the ratio between the tank and propellant masses m_t/m_p). The tankage fraction curves, obtained for the spherical titanium tank and corresponding to temperature of 45°C are presented in Figure 6.

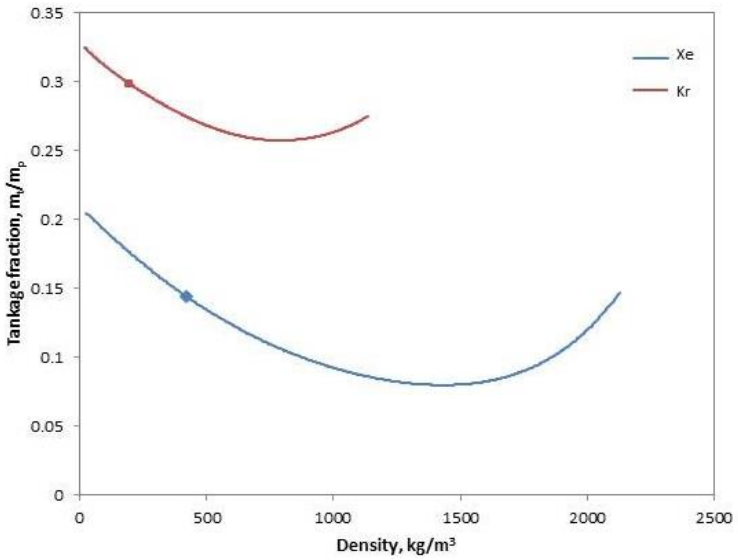

Figure 6: Tankage fraction vs propellant density for Xe and Kr at 45°C.

For the indicated maximal temperature the optimal propellant density, which would allow a minimization of the tankage mass fraction, would be 1141 kg/m^3 and 816 kg/m^3 for Xe and Kr respectively. These values were evaluated using the methodology described in [11]. However, as a result of the trade-off between the tank volume and mass, Xe and Kr are typically stored at 186 bar and 300 bar respectively. To illustrate the effect of the difference in storage conditions on the tank mass, the results of the corresponding tank parameters, estimated for a reference mission case of 50 MNs, operative point defined in Case 1, are presented in Table 6.

Table 6: Xe vs Kr titanium tank parameters comparison.

	Xe				**Kr**			
	Density, kg/m^3	**Tankage fraction m_t/m_p**	**Tank mass kg**	**Tank volume l**	**Density, kg/m^3**	**Tankage fraction m_t/m_p**	**Tank mass kg**	**Tank volume l**
Critical point	419 (58 bar)	-	-	-	192 (55 bar)	-	-	-
m_t/m_p optimized case	1141 at 94 bar	8.6%	175	1787	816 at 202 bar	25.7%	524	2497
P=186 bar	1884	10.3%	**209**	**1082**	751	25.7%	525	2715
P=300 bar	2128	14.7 %	299	958	1134	27.5%	**561**	**1798**

The estimated titanium tank mass for Xe shall be of 209 kg versus 561 kg for Kr, and the tank volume shall be of 1082 l (Xe) versus 1798 l (Kr). This means that much heavier and more voluminous tanks are necessary to store the same mass of propellant.
The implementation of the composite overwrapped (COPV) tanks allows to reduce slightly the tankage fraction and, therefore, the mass of the tanks. Based on the available heritage, the corresponding typical COPV tankage fraction for Xe is about 8% and for Kr is about 17%. The results of the corresponding COPV tank mass is presented in Table 7.

Table 7: Xe vs Kr COPV tank parameters comparison.

Xe	**Kr**

	Density, kg/m^3	Tankage fraction m_t/m_p	Tank mass kg	Density, kg/m^3	Tankage fraction m_t/m_p	Tank mass kg
P=186 bar	1884	8%	**163.1**	751	21%	346.6
P=300 bar	2128	9%	183.5	1134	17%	**428.1**

V.Architecture comparison results

In this section, the main results obtained by the previously introduced comparisons are described. First of all, the Analytical Hierarchy Process (AHP) with MonteCarlo weight derivation exploited for the comparison of the cases under analysis is presented. Then, the results obtained with MAGENTO tool and compared are presented for the all architecture cases introduced investigated for both sets of thruster operative points.

A. Trade-off weight definition

The trade-off methodology introduced follows the classical Analytical Hierarchy Process (AHP) where alternatives are compared through defined FoM for which weights and trade-off directions are assigned. Specifically, the FoM were selected considering the main parameters which intrinsically characterized the systems under analysis. The AHP proceeds with the definition of trade-off weight for each FoM, usually selected between 1 and 9, with respect to the lower of higher importance of the FoM, respectively. A MonteCarlo process was implemented to assess the interdependency among the FoM weights. This implies to define a range of values for each weight varying between a minimum weight value up to a maximum desire value. Lastly, the direction of the FoM depends on the desire to minimize or maximize the FoM value. As a result, in Table 8, all the FoMs, weights, directions and assumptions made are reported. Moreover, the FoM related to each comparison under analysis are identified since not all of them were evaluated for each comparison.

Table 8: weight ranges, directions and, main assumptions considered for each FoM;

Figure of Merit	Weight		Direction	Assumptions	MON vs CLU	PPU vs DDU	Xe vs Kr	ALL
	MIN	*MAX*						
S/C DRY MASS	8	9	LOW	▪ EPS string mass breakdowns of both HT20k and HT5k thruster-based system; ▪ ESA margin philosophy considered due to the preliminary level of the spacecraft design phase;	X	X	X	X
PROPELLANT MASS	8	9	LOW	▪ The propellant mass affects the design of the storage tank, as described in XXX;	X	X	X	X
TOTAL POWER	6	8	LOW	▪ Evaluate through MAGNETO; ▪ This FoM considers the power required by the space tug during nominal thrusting operations which represents the higher power demand case;		X	X	X

TOTAL TRANSFER TIME	7	9	LOW	▪ Evaluated through MAGNETO trajectory propagation module; ▪ This FoM was introduced in order to assess the minimum period of time required between two consecutive satellite transfers.	X	X	X	X
OUTWARD TRANSFER TIME	8	9	LOW	▪ Evaluated through MAGNETO trajectory propagation module; ▪ This FoM as introduced because of particular interest for the costumers which prefer reducing the period of time between the satellite launch and its entering in service.	X	X	X	X
DELTA-V	5	6	LOW	▪ Evaluated through MAGNETO trajectory propagation module; ▪ Defined steering control law based on weights calculated for each orbital element, as described in XXX;	X	X	X	X
THRUSTER COST	7	8	LOW	▪ Hofer's cost model [5]; ▪ Different EPS string components, EPS string baseline cost and, cost growth trend with respect the increasing of EPS power level;	X			X
PROPELLANT COST	7	8	LOW	▪ This FoM, evaluated through the orbit propagation module of MAGNETO tool was of particular interest due to the intrinsic characteristics of the space tug operation. In fact, to allow multiple transfers, the propellant mass shall be minimized as much as possible. ▪ The main assumption, already mention in Mission Definition section, is on the adoption of an ORS to refuel the space tug during the waiting period after each round trip.			X	X
THRUSTER RELIABILITY	6	9	HIGH	▪ A fixed EPS string reliability was assumed (R=0.95); ▪ A "k out of n" model was implemented to assess the reliability of the EPS; ▪ No redundant thrusters were considered;	X			X

TRL	7	9	HIGH	▪ This TRL was considered in order to catch the effort necessary to bring a particular technology considered up to space proven status;		X		X
COMPLEXITY	6	8	LOW	▪ This FoM was evaluated taking into account the complexity of system (i) integration, (ii) validation and, (iii) operation for both architectures;	X	X		N/A

Equation (2) was implemented to derive the weight of each FoM considering the MonteCarlo approach.

$$W_h = \frac{\sum_{k=1}^{N}\left(\frac{rand\left(W_{\min|i}, W_{\max|i}\right)_k}{\sum_{q=1}^{M} rand\left(W_{\min|i}, W_{\max|i}\right)_q}\right)}{N} \quad (2)$$

where N is the number of MonteCarlo random cases, M is the FoM index and W is the weight calculated for each h-th FoM.
The final scoring for the two architecture is obtained with the following expression:

$$S_i = \sum_{h=1}^{M} \delta_h \cdot W_h \cdot V_{hi} \quad (3)$$

where S_i represents the final score of the i-th case under comparison, δ_h is the direction of trade-off defined for each h-th FoM,V_{hi} is the i-th FoM normalized value.

B. SET1 of operative points: architecture comparison results

In this section, the comparison of the four architecture cases are reported with respect to the FoM identified in the previous section.
First, the comparison between monolithic and cluster architecture is shown in Table 9. As expected, the S/C dry mass for cluster architecture is greater than the mass of the monolithic ones, due to the greater number of components. Therefore, the cluster approach results also in a greater propellant mass, transfer times and thruster costs. The delta-V value for this architecture is slightly lower. On the other hand, the reliability is higher than the reliability of the monolithic architecture. In fact, the higher number of components allows to mitigate one or multiple failures with respect to the fulfilment of the mission requirements.

Table 9: Monolithic vs Cluster, SET-1 operative points, comparison results.

EPS architecture	**Monolithic**	**Cluster**
EPDCS architecture	**PPU**	PPU
Propellant typology	**Xe**	Xe
S/C dry mass, kg	**882,0**	1051,6
Propellant mass, kg	**801,3**	876,6
Total transfer time, days	**277,2**	302,6
Outward transfer time, days	**214,7**	228,5
Delta-V, m/s	**9179,8**	9177,4
Complexity	**1**	4
Thruster Cost, M€	**8**	15,9

Reliability	**0,95**	0,99
Final rank	**-0,3025**	-0,4317

Then, the comparison between PPU and DDU architecture was performed. In this case, different figures of merit were considered in order to highlight advantages and disadvantages of the two architectures under analysis. In particular, owing to the simplification of the PPU and the benefits obtained by the adoption of high-voltage bus, the S/C dry mass decrease of around 10% for the DDU architecture. The mass reduction implies a reduction of the propellant mass as well as the transfer times. Moreover, the total power budget for DDU is lower owing to the higher efficiency of the DDU in providing power to the thruster. However, the TRL, which identified the technological maturity, shows how the DDU needs a further development to be efficiently implies.

Table 10: PPU cs DDU, SET-1 operative points, comparison results.

EPS architecture	Monolithic	**Monolithic**
EPDCS architecture	PPU	**DDU**
Propellant typology	Xe	**Xe**
S/C dry mass, kg	882,0	**806,5**
Propellant mass, kg	801,3	**766,9**
Total Power, W	25607,3	**24359,6**
Total transfer time, days	277,2	**265,2**
Outward transfer time, days	214,7	**208,2**
Delta-V, m/s	9179,8	**9178,9**
Complexity	1	**0,5**
TRL	9	**5**
Final rank	-0,3763	**-0,3561**

The last comparison for the first set of operative point is related to the possibility to operate with Krypton instead of Xenon. The higher tank fraction (see section III) and the higher discharge power of the selected operative point results in higher dry mass of the spacecraft, which decrease the thrust over mass ratio. As a consequence, an increment of around 9 % occurs for all the FoM under analysis. However, the main advantages in the adoption of Krypton is the reduction of the propellant cost of over 90 %. This allows to identify the adoption of Krypton as the optimal solution.

Table 11: Xe vs Kr, SET-1 operative points, comparison results.

EPS architecture	Monolithic	**Monolithic**
EPDCS architecture	PPU	**PPU**
Propellant typology	Xe	**Kr**
S/C dry mass, kg	882,0	**1010,4**
Propellant mass, kg	801,3	**859,6**
Total Power, W	25607,3	**27432,7**
Total transfer time, days	277,2	**297,2**
Outward transfer time, days	214,7	**225,7**
Delta-V, m/s	9179,8	**9178,2**
Propellant cost, m€	1,763	**0,103**
Final rank	-0,5522	**-0,4406**

C. SET2 of operative points: architecture comparison results

In this section, the comparison between the alternative architectures previously introduced and analysed with the second set of operative points is reported.

First, the comparison between cluster and monolithic shows how the latter case represents the optimal architecture to implement if the second set of operative points is considered. The results are reported in Table 12. In this case, the higher advantage is gained with the reduction of propellant mass. In fact, the specific impulse for this architecture

second set of operative points is reduced to 2130s which increases the propellant mass of 140 kg. Furthermore, the higher wet mass of the spacecraft results in a higher transfer time which for the cluster architecture results to be around 287 days.

Table 12: Monolithic vs Cluster, SET-2 operative points, comparison results.

EPS architecture	**Monolithic**	Cluster
EPDCS architecture	**PPU**	PPU
Propellant typology	**Xe**	Xe
S/C dry mass, kg	**882,0**	935,6
Propellant mass, kg	**801,3**	1016,8
Total transfer time, days	**277,2**	287,5
Outward transfer time, days	**214,7**	220,1
Delta-V, m/s	**9179,8**	9180,4
Complexity	**1**	4
Thruster Cost, M€	**8**	15,9
Reliability	**0,95**	0,99
Final rank	**-0,2359**	-0,3697

The DDU architecture of the EPDCS results as the optimal design solution even for the second set of operative points. Even for this comparison, same considerations can be done on the advantages in the adoption of DDU architecture. With respect to the first set of points, propellant mass, transfer times and the delta-V values are slightly lower due to the higher values of both thrust and specific impulse. However, the selected operative point corresponds to a higher discharge power to be fed to the thruster. Therefore, a higher value of total power and dry mass are obtained.
The results of the comparison are shown in Table 13.

Table 13: PPU vs DDU, SET-2 operative points, comparison results.

EPS architecture	Monolithic	**Monolithic**
EPDCS architecture	PPU	**DDU**
Propellant typology	Xe	**Xe**
S/C dry mass, kg	882,0	**835,2**
Propellant mass, kg	801,3	**762,1**
Total Power, W	25607,3	**25048,6**
Total transfer time, days	277,2	**253,3**
Outward transfer time, days	214,7	**197,9**
Delta-V, m/s	9179,8	**9175**
Complexity	1	**0,5**
TRL	9	**5**
Final rank	-0,3763	**-0,3553**

The last comparison was performed between the alternative propellant selection as shown in Table 14. Even in this case, the optimal solution was found in the adoption of the Krypton for the operation of the thruster. The high value of specific impulse (around 3000s) allows to reduce the propellant mass of over 180 kg with respect the propellant mass derived with 2500s of the first set of Krypton operative point. This reduction also affects the dry mass of the spacecraft, for example due to the reduction of the tank mass. However, the lower thrust level, equal to 0,77 N, causes an increasing of the transfer times of around 20%, delaying the delivering of the satellite on its operative orbit and extending the period between due to consecutive transfers. Even under those circumstances, the main contribution in the final result is given by the krypton cost of over 1,6 M€ lower with respect to the Xenon.

Table 14: Xe vs Kr, SET-2 operative points, comparison results.

EPS architecture	Monolithic	**Monolithic**
EPDCS architecture	PPU	**PPU**
Propellant typology	Xe	**Kr**

S/C dry mass, kg	882,0	**935,7**
Propellant mass, kg	801,3	**671,9**
Total Power, W	25607,3	**25607,3**
Total transfer time, days	277,2	**361,7**
Outward transfer time, days	214,7	**276,8**
Delta-V, m/s	9179,8	**9177,8**
Propellant cost, m€	1,763	**0,081**
Final rank	-0,5522	**-0,4415**

D. Comparison among all cases

The comparison among all the architecture alternatives analysed, with respect to the two sets of operative points, results in the identification of the system based on krypton operation as the optimal architecture to adopt for the space tug system. In particular, the operative point at 1N, 2500s and 22.5 kW demonstrated a lower propellant mass, transfer times and propellant cost. The latter parameter plays the grater role in the selection of this case owing to a saving of over 1.6 M€ with respect to the baseline case.

Table 15: comparison of all the cases under analysis.

Operative Points	EPS architecture	EPCDS architecture	Propellant	SCORE	RANK
SET_1	Monolithic	PPU	Xe	-0,07068	5
	Monolithic	**PPU**	**Kr**	**-0,06532**	**1**
	Monolithic	DDU	Xe	-0,0703	3
	Cluster	PPU	Xe	-0,09218	6
SET_2	Monolithic	PPU	Xe	-0,07068	5
	Monolithic	PPU	Kr	-0,06596	2
	Monolithic	DDU	Xe	-0,07007	4
	Cluster	PPU	Xe	-0,09317	7

VI.CONCLUSION

In this paper, a space tug was envisaged to provide transfer service of commercial telecommunication satellite up to the geostationary orbit (GEO). This reference scenario was selected to investigate the adoption of technologies alternative to those currently exploited. The main purpose of the research is to investigate the possibility to mitigate several criticalities of these typologies of transportation systems, mainly related to both mass and power budgets.

The analysis performed considers a trade-off between the adoption of a monolithic architecture based on a single 20 kW EPS and a cluster architecture based on multiple 5 kW EPS strings.
The propellant comparison encompasses several aspects i.e. HT performance, propellant storage conditions, tank size and volume, propellant cost and system complexity. All these factors have been evaluated comparing xenon, which is already largely used, and krypton, owing to its advantages in lower price with respect to xenon with comparable performance.
The last analyses performed at system level considers the comparison between the architecture of the EPS based on a power-processing unit (PPU) and the direct-drive (DD) approach. The latter solution allows to deliver power to the thruster directly from the solar arrays, without the need of a heavy and bulky PPU, in particular for HP-SEP. However, the implementation of a DD approach requires to develop satellite platforms with high bus voltages.

In order to investigate the various system parameters and verified the fulfilment of mission requirements and constrains, the MISS tool was updated implementing the possibility to implement DDU and alternative propellant operation. The new MAGNETO tool allows to evaluate different architecture alternatives with respect to the mission

needs. The eight reference cases were chosen for the comparison of possible high-power space tug system architectures. These cases were investigated considering two different approaches for the selection of the thruster operative points. Through a trade-off analysis based on pre-determined figures of merit, the optimal solution was identified for both sets. The optimal solution was identified as the system based on a monolithic 20kW EPS string operating with a traditional PPU and krypton propellant.
Further development of this analysis will be implemented also investigating other architecture alternatives. Moreover, a greater number of the operative points will be compared, based on the experimental verification of the thruster performance maps, foreseen in SITAEL in the nearest future.

Acknowledgments

The work described in this paper has been funded by the European Union under H2020 Programme CHEOPS-GA 730135 and by the European Space Agency under GSTP Programme, Contract 4000122232.

References

[1] Andreussi, T., Piragino, A., Ferrato, E., Reza, M., Faraji, F. Beccati, G., Pedrini, D., Kitaeva, A., Andrenucci, M., "HT20k Hall thruster development status", *69th International Astronautical Congress (IAC)*, Bremen, Germany, October 2018.

[2] Ducci, C., Arkhipov, A., Andrenucci, M., "Development and performance characterization of a 5 kW class Hall-effect thruster", IEPC-2015-215,/ISTS-2015-b-215.

[3] Mammarella, M., Paissoni, C.A., Fusaro, R., Viola, N.,Andreussi, T., Andrenucci, M., "A 20kW-class Hall Effect Thruster to Enhance Presenta ns Future Space Missions", *69th International Astronautical Congress (IAC)*, Bremen Germany, October, 2018.

[4] Paissoni, C.A., Mammarella, M., Fusaro, R., Viola, N., Andreussi, T., Rossodivita, A., Saccoccia, G., "Deep Space transportation enhanced by 20kW-class Hall Effect Thruster", *69th international Astronautical Congress (IAC)*, Bremen, Germany, October, 2018.

[5] ISECG, "Global Exploration Roadmap", 2018.

[6] Rimani, J., Paissoni, C.A., Viola, N., Gonzalez del Amo, J., Saccoccia, G., "Multidisciplinary Mission and System Design Tool for a Reusable Electric Propulsion Space Tug", *11th IAA Symposium on the Future of Space Exploration: Moon, Mars and Beyond: Becoming and Interplanetary Civilization*, Turin, 2019.

[7] Qaise, O., Moorhouse,A., Birreck,D., "Operational Concept of the First Commercial Small-Geo Based Mission," Proceedings of SpaceOps 2012, *The 12th International Conference on Space Operations*, Stockholm, Sweden, 2012

[8] Luebberstedt, H., et al. "Electra–Full Electric Propulsion Satellite Platform for GEO Missions.", 2017.

[9] Herron, B.G., and Opjordan, "High Voltage Solar Arrays with Integral Power Conditioning," *AIAA 8th Electric Propulsion Conference*, AIAA Paper 1970-1158.

[10] Andreussi, T., Saravia, M.M., Ferrato, E. Piragino, A., Rossodivita, A., Andrenucci, M., Estublier, D. "Evaluation and Testing of Alternative Propellants for Hall Effect Thrusters", IEPC-2017-380, *35th International Electric Propulsion*, 2017.

[11] Parissenti, G., Koch, N., Pavarin, D., Ahedo, E., Katsonis, K., Scortecci, F., Pessana, M. "Non-conventional propellants for electric propulsion applications", *Space Propulsion 2010*, 1841086.

[12] Welle R.P., "Propellant Storage Considerations for Electric Propulsion", IEPC-91-107, *22nd International Electric Propulsion Conference*, Viareggio, Italy.

[13] Shagayda, A.A. "On Scaling of Hall Effect Thrusters", IEPC-2013-056, *33rd International Electric Propulsion Conference*, Washington DC, USA, 2013.

[14] Wertz, J. R., Everett, D.F., Puschell, J.J., "Space mission analysis and design", Space technology Library, 2011.

[15] Metcalf, K.J., "Power Management and Distribution (PMAD) Model Development", Report contract NAS2-01140

[16] Spence, B., White, S., Wilder, N., Gregory, T., Douglas, M., Takeda, R., "Next Generation UtraFlex solar array for NASA's New Millennium Program Space Technology 8", IEEE *Aerospace Conference Proceedings*, 2005

[17] Mercer, C. R., Kerslake, T. W., Scheidegger, R. J., Woodworth, A. A., & Lauenstein, J. M., "Solar Electric Propulsion Technology Development for Electric Propulsion", *Space Power Workshop*, Huntington Beach, CA, 2015.

[18] Zubi, G., Dufo-López, R., Carvalho, M., & Pasaoglu, G. "The lithium-ion battery: state of the art and future perspectives", Renewable and Sustainable Energy Reviews, 89, 292-308, 2018.